ISSN 8756-6990, Optoelectronics, Instrumentation and Data Processing, 2021, Vol. 57, No. 3, pp. 232–239. © Allerton Press, Inc., 2021.
Russian Text © The Author(s), 2021, published in Avtometriya, 2021, Vol. 57, No. 3, pp. 10–18.

ANALYSIS AND SYNTHESIS OF SIGNALS AND IMAGES

Space-Time Signals and Their Filtering in Radio-Frequency Engineering Systems with Antenna Arrays under Conditions of Active Interference

A. A. Murasev[1*] and A. A. Spektor[1]

[1] *Novosibirsk State Technical University, Novosibirsk, 630073 Russia*

Received March 4, 2021; revised April 1, 2021; accepted April 8, 2021

Abstract—A method is proposed for active interference suppression based on the difference in the spectral characteristics of space-time signals and interference in radio-frequency engineering systems with antenna arrays. An expression for the spectrum of the space-time signal on a linear antenna array is obtained. The results of the experimental study of the developed algorithm for a number of sources of active interference are presented.

DOI: 10.3103/S8756699021030122

Keywords: *space-time signals, antenna arrays, active interference, matched filtering*

1. INTRODUCTION

With the development of digital technologies, antenna arrays (AAs) are increasingly used to improve the efficiency of the developed systems. They are used not only in radio-frequency engineering systems [1–5] but also in image processing [6].

Their use in radiolocation and communication creates conditions for a significant improvement of characteristics of radio-frequency engineering systems and expansion of their functionality. This is due to the potential ability to flexibly control the directional characteristics and provide a better solution to the problems of the radio-frequency engineering system. The most important application is the struggle against external active interference radiated, in the general case, by mobile sources from arbitrary points of space. The presence of powerful active interference makes it impossible to use the known methods [7, 8] for a high-quality target detection.

Increasing interest in AAs is associated with the development of digital control technologies of radio-frequency engineering systems. In modern radar systems, the structural element of which is the transceiver module (TM), a digital signal, when received, is generated at the intermediate frequency at the output of the antenna array, because there is an analog-to-digital converter (ADC) in each receiving channel. The signals in radiation mode are also controlled by digital methods. In this regard, the antenna arrays of modern radars are called digital AAs (DAAs).

The dominant approach to optimizing radio reception in the presence of active interference is to find the optimal weighting coefficients in the generation of the total signal to obtain the best signal-interference characteristics by forming an optimum antenna pattern (OAP). A number of studies [1–3] are known that develop this principle. For Gaussian interference distribution, its use leads to the formation of a decisive statistic in the form of a quadratic form for the signal vector, the core of which is the inverse correlation matrix of the total interference. The sizes of the observed signal vector and the matrix are determined by the product of the number of antenna elements by the number of time samples of the signals involved in the processing. This is usually a huge value, which hinders the use of this approach. Numerous studies are aimed at overcoming the problem by finding a variety of simplifications,

*E-mail: alex190789@gmail.com

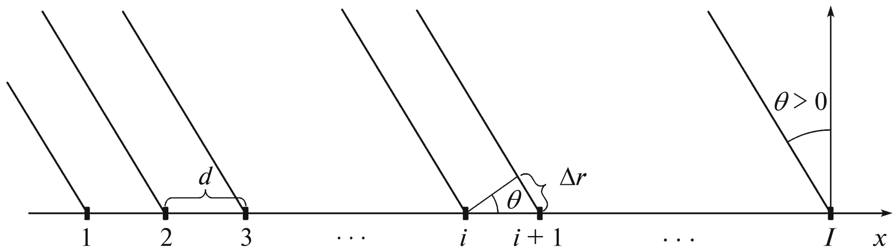

Fig. 1. Geometry of the linear equidistant array.

approximations, etc. Impressive successes have been achieved in this way, which, however, does not exhaust the problem.

In this article, we propose a different approach, the basis of which is the optimization of radio reception of space-time signals generated in the form of a sequence of digital frames. A similar approach, presented, e.g., in [4], is developed here in relation to the description and filtering of signals and interference in systems with a linear digital antenna array (LDAA) and can be extended to surface AAs.

2. SIGNALS AND INTERFERENCE IN A SYSTEM WITH THE LDAA AS 2D SPACE-TIME SIGNALS

Let us consider signals and disturbances that have a flat wavefront on the receiving AA. It is accepted to consider them as narrow-band oscillations if the following condition is true

$$\nu = \Delta f/\bar{f}_0 \ll 1, \tag{1}$$

where Δf is the width of the spectrum of the signal or interference and $\bar{f}_0$ is the average frequency value. The fulfillment of condition (1), however, does not mean that the signal is narrowband in the spatial sense. The signal is also narrowband in the spatial sense if, over the LDAA with a length of l_{aa}, the difference of phase incursions for the spectrum boundary frequencies $f_0 + \Delta f/2$ and $f_0 - \Delta f/2$ meets the condition $2\pi\Delta f l_{\text{aa}}/c \ll 2\pi$ (c is the wave propagation speed), i.e., when $\Delta f \ll c/l_{\text{aa}}$. In the opposite case, when $\Delta f \sim c/l_{\text{aa}}$, the signals satisfying narrow-band condition (1) acquire broadband properties for the AA aperture, and they are considered broadband in the spatial sense [5]. The need for the analysis of such situations increases due to the use of more and more broadband modulation types in modern radio-frequency engineering systems.

Let us represent a narrowband oscillation by the following expression

$$u(t) = U(t)\cos[\omega_0 t + \psi(t)], \tag{2}$$

where $\omega_0 = 2\pi f_0$ and $U(t)$ and $\psi(t)$ are the functions describing the amplitude and angle modulation of the deterministic signal or the amplitude and phase fluctuations of the narrowband interference.

Figure 1 illustrates the generation of a spatial signal when receiving on a linear antenna array with I equidistant elements located along the x axis. The angle of arrival of the signal is counted from the normal to the x axis, and the counterclockwise motion is considered positive. The signals received by the different elements of the linear antenna array (LAA) differ in time delays. At an arbitrary angle of arrival θ, the value of the delay of signals on neighboring elements is as follows

$$\tau_0 = \frac{\Delta r}{c} = \frac{d\sin\theta}{c}. \tag{3}$$

As a rule, the distance between the elements of AAs is selected from the condition $d = \lambda/2$; then,

$$\tau_0 = \frac{\lambda\sin\theta}{2c} = \frac{\sin\theta}{2f_0},$$

where $\lambda = c/f_0$ is the wavelength corresponding to the frequency f_0.

The set of time signals on the I receiving elements can be regarded as a space-time signal

$$u(t,i) = U(t-(i-1)\tau_0)\cos[\omega_0(t-(i-1)\tau_0) + \psi(t-(i-1)\tau_0)], \quad i = \overline{1,I}, \tag{4}$$

whose arguments are time t and discrete spatial coordinate i. Time-space signal (4) actually consists of I identical time signals (2) with different time delays, but their aggregate contains directional information which is missing in the individual time signals. The delays of the signals on the different LAA elements are counted from the first element $i = 1$, and expression (2) describes the signal on this element of the AA. Introducing a continuous coordinate x (see Fig. 1), we define the following time delay for its arbitrary value

$$\tau(x) = \frac{x}{d}\tau_0 = \frac{x \sin\theta}{c} = k(\theta)x$$

and generate a 2D continuous signal

$$u(t, x) = U(t - k(\theta)x) \cos[\omega_0(t - k(\theta)x) + \psi(t - k(\theta)x)], \ x \in [-x_{\rm m}/2, x_{\rm m}/2], \tag{5}$$

where $k(\theta) = \sin\theta/c$ is the coefficient of proportionality between space and time variables depending on the angle θ and $x_{\rm m}$ is the linear size of the grid, and the origin of coordinates along the x axis is moved to the midpoint of the LAA. At discrete spatial points $x = i\tau_0$ the continuous signal (5) coincides with (4), which makes it possible to consider (4) to be a result of spatial discretization (5) or (5) to be a result of spatial interpolation (4).

Performing time sampling with the step of Δt, we generate a 2D discrete (and at level quantization, digital) signal from (4)

$$u(l, i), \quad l = \overline{1, L}, \quad i = \overline{1, I},$$

each row l of which corresponds to a fixed point in time $t_l = (l - 1)\Delta t$ and each column i, to a certain AA element. In the case of a pulse signal, the duration of the analysis interval $T_{\rm a} = (L - 1)\Delta t$ can be determined by the signal duration. As a result, a 2D signal is generated, a discrete or digital frame with a size of $L \times I$ elements. Significant reduction in size is achieved by digitizing signals in receivers at an intermediate frequency.

Let us consider characteristic features of spatial properties of a 2D signal. For this purpose, by fixing the time $t = \hat{t}$, let us represent the spatial section of signal (5) as follows

$$u(\hat{t}, x) = U(\hat{t} - k(\theta)x) \cos[\omega_0(k(\theta)x - \hat{t}) - \psi(\hat{t} - k(\theta)x)], \ x \in [-x_m/2, x_m/2]. \tag{6}$$

Expression (6) describes a quasiharmonic oscillation of the spatial frequency $\omega_{\rm s0}(\theta) = \omega_0 k(\theta)$, which depends on the angle of arrival of the wave θ. The amplitude $U(\cdot)$ and the phase $\psi(\cdot)$, which also depend on x, change by ν^{-1} times slower, and the changes are relatively small at a finite-size LAA. Thus, assuming that the frequency bandwidth of interference at the ADC input coincides with the signal bandwidth Δf, we estimate its time correlation interval as $\tau_t \sim 1/\Delta f$. In this case, the spatial correlation interval

$$\tau_x \sim \tau_t/k(\theta) = c/(\Delta f \sin\theta)$$

is minimum at $\theta \to 90°$ and increases infinitely if the interference is from $\theta \sim 0°$. For a bandwidth of $\Delta f = 100$ MHz, we have an estimate of $\tau_x \sim 3/\sin\theta$ (m). This estimate, depending on θ, is either commensurate with the size of the antenna (and in this case the interference is a broadband signal in the spatial sense) or significantly exceeds it. Figure 2 presents a qualitative view of spatial signal (6), where modulation changes in amplitude and phase are not reflected, and their values in the figure are selected different for clarity. The monotonic change in the oscillation frequency from zero for $\theta = 0$ to maximum for $\theta = 90°$ is characteristic. The data in Fig. 2 correspond to the LAA containing $I = 70$ receiving elements located at a distance $d = \lambda/2$.

A 2D spectral analysis of 2D space-time signals can be one of the methods for studying them. The 2D spectrum of the signal $u(t, x)$ is defined by the following expression [4, 9, 10]

$$\dot{U}(\omega_t, \omega_x) = \int_{-\infty}^{\infty} \int_{-x_m/2}^{x_m/2} u(t, x) \mathrm{e}^{-j\omega_t t - j\omega_x x} \, dt \, dx, \tag{7}$$

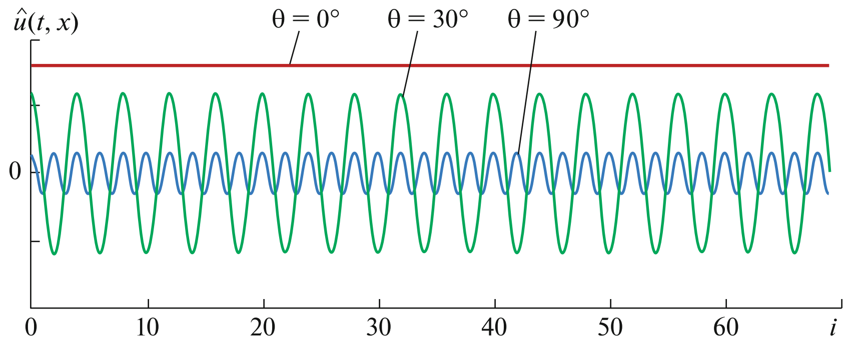

Fig. 2. View of the spatial signal on a linear antenna array.

in which $\omega_t = 2\pi f_t$ and $\omega_x = 2\pi f_x$ are the frequencies corresponding to time and space oscillations and called further as time and space frequencies. The 2D LAA signal is characterized by the following property

$$u(t,x) = u(t - k(\theta)x),$$

with which it is not difficult to obtain from (7)

$$\dot{U}(\omega_t, \omega_x, \theta) = \int_{-\infty}^{\infty} \int_{-x_m/2}^{x_m/2} u(t - k(\theta)x)^{-j\omega_t t - j\omega_x x}\, dt\, dx$$

$$= \dot{U}(\omega_t) x_{\mathrm{m}} \frac{\sin[(\omega_t k(\theta) + \omega_x) x_{\mathrm{m}}/2]}{(\omega_t k(\theta) + \omega_x) x_{\mathrm{m}}/2}, \qquad (8)$$

where $ds\dot{U}(\omega_t) = \int_{-\infty}^{\infty} u(t) e^{-j\omega_t t}\, dt$ is the usual spectrum of the signal $u(t)$ (2). As the antenna size x_{m} increases, in the limit from (8) we find

$$\dot{U}(\omega_t, \omega_x, \theta) \xrightarrow[x_{\mathrm{m}} \to \infty]{} \dot{U}(\omega_t)\delta(\omega_t k(\theta) + \omega_x),$$

where $\delta(\cdot)$ is the delta function. The qualitative view of 2D spectrum (8) is shown in Fig. 3. The multiplier of the form $\sin(\cdot)/(\cdot)$ in (8) forms a nonzero band on the frequency plane along the line $\omega_x = -k(\theta)\omega_t$, whose width is determined by the antenna size x_{m} and whose position in the plane is determined by the angle of arrival of the wave θ. The 2D spectral function is focused at the intersection shown in Fig. 3 in gray. For different wave arrival angles, the position of the shaded areas is different, which can serve as a basis for signal separation and interference control.

The feature of the space-time signal generated by the internal noise of the receiving elements of the TM is due to their independence in the different channels. Therefore, the autocorrelation function of this signal is described by the following expression

$$B(\tau_t, \tau_x) = DR(\tau_t)\delta(\tau_x),$$

where τ_t and τ_x are time and space shifts, D is the dispersion, the same in all channels, and $R(\tau_t)$ is the normalized time function of noise correlation in each channel determined for the signal at the ADC input by the amplifier frequency response. A 2D power spectral density (PSD) of the internal noise is as follows

$$G(\omega_t, \omega_x) = \int_{-\infty}^{\infty} \int_{-\infty}^{\infty} B(\tau_t, \tau_x) e^{-j\omega_t \tau_t - j\omega_x \tau_x}\, d\tau_t\, d\tau_x = DG_t(\omega_t),$$

where $G_t(\omega_t)$ is the Fourier transform of $R(\tau_t)$. It follows that the PSD dependence on the time frequency ω_t is determined by the usual PSD of channel noise. The 2D PSD is a uniform function with respect to the spatial frequency ω_x.

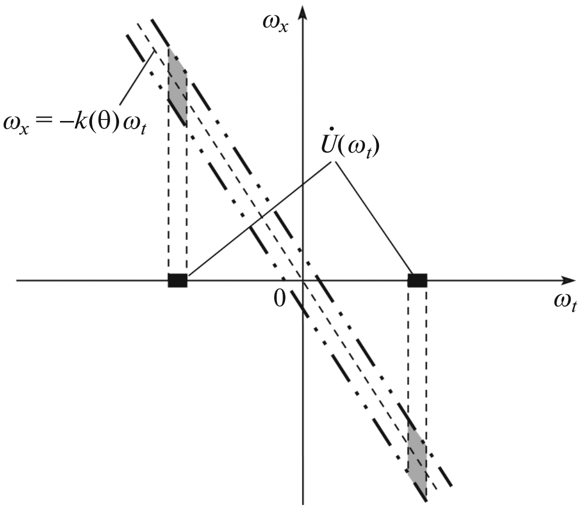

Fig. 3. Qualitative image of the 2D spectrum of the spatial temporal signal.

3. ADAPTIVE MATCHED FILTERING OF SIGNALS IN THE PRESENCE OF CONTINUOUS ACTIVE INTERFERENCE AND INTERNAL NOISE

Based on the spectral characteristics of signals and interference, different types of filtering can be performed. Since in the considered problem of active interference suppression the useful signal is a signal of known shape, this article considers the application of the 2D matched filtering.

For definiteness, we assume that the useful signal is a pulse with a linear frequency modulation (LFM) with a duration τ_{p} and frequency deviation f_{d}. The direction of signal arrival is determined by the angle θ_{s}, each of n active interference sources is characterized by the angle of arrival $\theta_{\text{a}i}$. The signal power at the ADC input is $P_{\text{s in}}$, the noise power in the signal frequency band f_{d} is $P_{\text{int.input}i}$, $i = \overline{1, n}$.

The transfer coefficient of the space-time filter matched with the signal is determined by the following expression

$$k(jf_t, jf_x, \theta_{\text{s}}, \boldsymbol{\theta}_{\text{int}}) = \frac{S^*(jf_t, jf_x, \theta_{\text{s}})}{\sqrt{G_\Sigma(f_t, f_x, \boldsymbol{\theta}_{\text{int}})}} e^{-j2\pi f_t \tau_{\text{p}} - j2\pi f_x x_{\text{m}}}.$$

Here, $S(jf_t, jf_x, \theta_{\text{s}})$ is the 2D spectrum of the useful signal depending on the expected signal arrival angle, $G_\Sigma(f_t, f_x, \boldsymbol{\theta}_{\text{a}})$ is the PSD of total interference including thermal noise of receivers depending on the vector of the arrival angles of active interference $\boldsymbol{\theta}_{\text{a}} = \|\theta_{\text{a}i}, i = \overline{1, n}\|$. The algorithm of 2D matched filtering contains the calculation of the 2D discrete spectrum of the signal $u(l, i)$, $l = \overline{1, L}$, $i = \overline{1, I}$:

$$\dot{U}(k, m) = \sum_{l=1}^{L} \sum_{i=1}^{I} u(l, i) e^{-j(2\pi lk/L + 2\pi im/I)},$$

its multiplication by coefficient (9) discretized by f_t and f_x transfer and inverse 2D Fourier transform. The delays in transfer coefficient (9) correspond to the maximum signal-to-noise ratio at the point $t = \tau_{\text{p}}$, $x = x_m$ of the 2D space.

This algorithm can be used in the adaptive form with a preliminary estimation of the PSD of interference $G_\Sigma(f_t, f_x, \boldsymbol{\theta}_{\text{a}})$. Obtaining its estimation (in contrast to the estimation of LFM signal parameters [11]) does not represent a fundamental problem [12, 13] if there are intervals in the radio system operation during which there is no useful signal. In many radio-frequency engineering systems such condition is quite possible. The volume of the training sample in the following results of the statistical experiment was 100 space-time frames of interference.

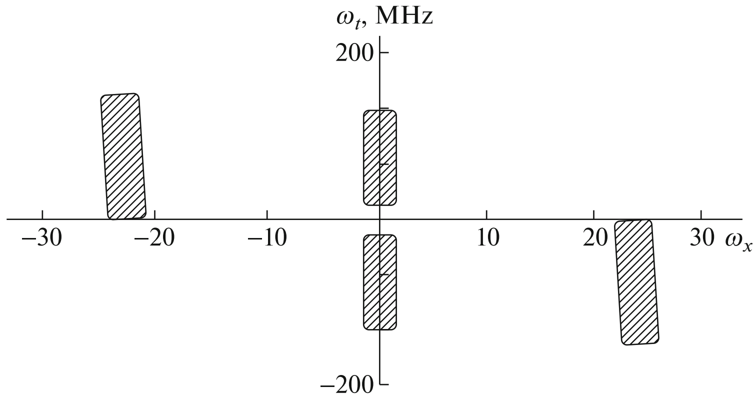

Fig. 4. Signal and interference spectral diagram ($n = 1$, $\theta_{\text{int}1} = 10°$, $q_{\text{s/int}} = 1$).

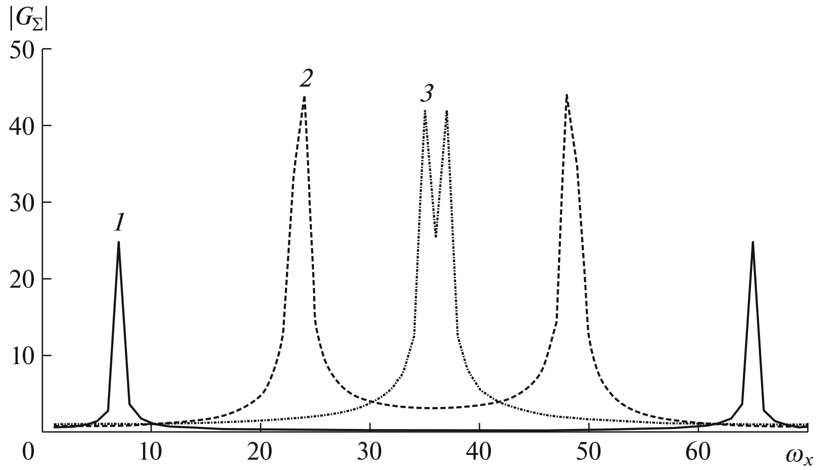

Fig. 5. Spatial interference spectrum for arrival angles: (*1*) $\theta_{\text{int}} = 10°$, (*2*) $\theta_{\text{int}} = 40°$, (*3*) $\theta_{\text{int}} = 80°$

4. RESULTS OF MODELING SPACE-TIME FILTERING

Filtering characteristics were studied by statistical modeling. A radar with a LAA with a size of $I = 70$ was considered using a pulsed radio signal with a duration of $\tau_{\text{p}} = 1$ μs with frequency deviation $f_{\text{d}} = 100$ MHz. Preprocessing in the TM was carried out in an intermediate frequency amplifier with an frequency response close to rectangular in the frequency band $\sim 1.1 f_{\text{d}}$ and a linear phase response. Spectral characteristics of interference and internal noise were generated in the same amplifier. A different number of active interference sources $n = \overline{1, 11}$ with different arrival angles $\theta_{\text{a}i}$, the signal arrival angle $\theta_{\text{s}} = 0$, were considered. The signal and interference energies were given by the ratios $q_{\text{s/int}i} = P_{\text{s}}/P_{\text{int}i}$, $i = \overline{1, n}$, powers of the signal P_{s} and interference $P_{\text{int}i}$, $i = \overline{1, n}$, and the relations $q_{\text{n/int}i} = P_{\text{n}}/P_{\text{int}i}$, $i = \overline{1, n}$, and noise power P_{n} (the same in all receiving channels) to the interference power.

Figure 4 shows the spectral diagram, a cross-section of the space-time spectrum of a mixture of signal and interference (one source of active interference) at an angle $\theta_{\text{int}1} = 10°$ by a plane parallel to the 2D frequency plane at half level for $q_{\text{s/int}1} = 1$, $q_{\text{n/int}1} = -40$ dB.

An idea of the blurring of the spectral characteristics is given by Fig. 5, which shows the spatial spectra of interference coming from different directions. At a low level, there are extended tails, which prevents the complete suppression of interference, even with significant differences in the angles of arrival of the signal and interference.

The filtering efficiency was evaluated by the change in the signal-to-noise ratio $\Delta q = q_{\text{out}} - q_{\text{in}}$ (dB) at the filter output with respect to its input for $q_{\text{s/int}i} = 1$ $\forall i$ for different values of $q_{\text{n/int}i}$. Figure 6 shows

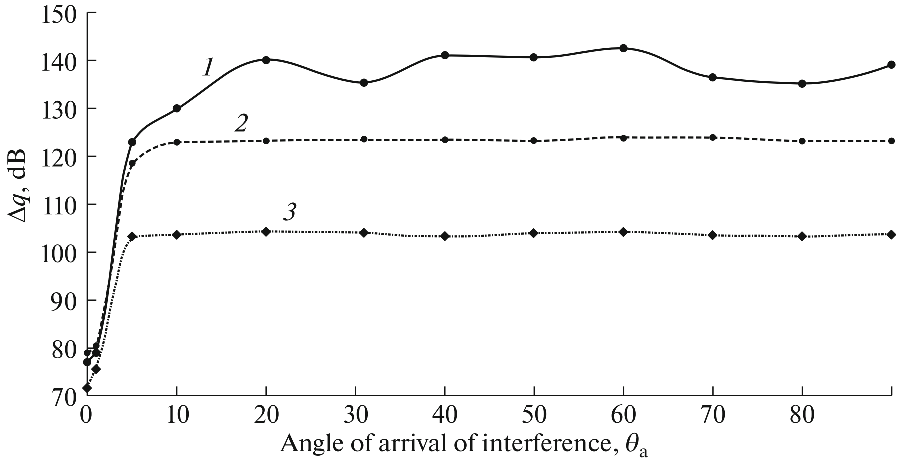

Fig. 6. Spatial interference spectrum for arrival angles: Dependences of the gain Δq on the angle of arrival of interference θa for different values of $q_{\mathrm{n/int}}$: −60 dB (*1*); −40 dB (*2*); and −20 dB (*3*).

the dependences of the gain Δq on the angle of arrival of interference (number of interference sources $n = 1$) for $\theta_{\mathrm{s}} = 0°$ and different ratios of intensities of external and internal interference $q_{\mathrm{n/int}}$. Increase in the number the internal noise of the receiving devices significantly reduces the magnitude of the gain.

The effect of the number of active interference sources with different spatial locations was studied. In the presence of 11 interference sources with angles $\boldsymbol{\theta}_{\mathrm{int}} = \{5, 10, 15, 20, 25, 30, 40, 50, 60, 70, 80\}°$ for $\theta_{\mathrm{s}} = 0°$ and $q_{\mathrm{n/int}} = -40$ dB, the gain was 116 dB, which, as seen in Fig. 6, is only 1–2 dB less than the case of a single source with an arrival angle of $\theta_{\mathrm{a}} = 5°$.

5. CONCLUSIONS

The approach proposed in this article to attenuate the effects of external active interference relies on the representation of the input data as space-time signals. In the considered variant of the linear grid, the signals are 2D. Their processing consists in calculating the 2D Fourier transform, multiplying by the frequency transfer coefficient, and the reverse 2D Fourier transform. Methods of 2D transforms are well developed [14, 15], their computational labor intensity is estimated by the values of $N \log_2 N$ of operations of multiplication and $(N/2)\log_2 N$ operations of summation when processing frames with a size $N = L \times I$ elements. The results of the study of the processing testify to the high efficiency of interference suppression, the decrease of which is relatively small when the number of active interference sources increases.

Further development of the approach can be directed to the development of the method as applied to the antenna arrays of other types, in particular the planar antenna arrays in radio systems with broadband signals.

REFERENCES

1. D. I. Voskresenskii and A. I. Kanashchenkov, *Active Phased Antenna Array* (Radiotekhnika, Moscow, 2004).
2. R. A. Mozingo and T. W. Miller, *Introduction to Adaptive Arrays* (Wiley, New York, 1980).
3. M. V. Ratynskii, *Adaptation and Superresolution in Antenna Arrays* (Radio i Svyaz', Moscow, 2003).
4. D. E. Dudgeon and R. M. Mersereau, *Multidimensional Digital Signal Processing* (Prentice Hall, Englewood Cliffs, N.J., 1984).
5. *Signal Processing in Radioengineering Systems*, Ed. by A. P. Lukoshkin (Leningrad. Univ., Leningrad, 1987).
6. V. P. Yushchenko, V. G. Edvabnik, O. V. Gofman, T. V. Duluba, and V. N. Legkii, "Method of object image reconstruction using a circular antenna array," Optoelectron., Instrum. Data Process. **56**, 614–622 (2020). https://doi.org/10.3103/S8756699020060151
7. I. F. Lozovskii, *Digital Signal Processing in Surveillance Radar* (Novosibirsk Gos. Tekh. Univ., Novosibirsk, 2016).

8. V. K. Klochko, “Detection of moving objects by a passive scanning system,” Optoelectron., Instrum. Data Process. **55**, 59–65 (2019). https://doi.org/10.3103/S8756699019010102
9. K. K. Vasil’ev, V. A. Kazakov, A. A. Spektor, and A. P. Trifonov, *Applied Theory of Random Processes and Fields* (Ulyanovsk Gos. Tekh. Univ., Ulyanovsk, 1995).
10. I. S. Gruzman, V. S. Kirichuk, V. P. Kosykh, G. I. Peretyagin, and A. A. Spektor, *Digital Image Processing in Information Systems: Textbook* (Novosibirsk Gos. Tekh. Univ., Novosibirsk, 2002).
11. V. A. Shcherbachev, “Estimating the frequency parameters of LFM signal by a sample of increasing size,” Optoelectron., Instrum. Data Process. **57**, 1–7 (2021). https://doi.org/10.3103/S8756699021010106
12. S. L. Marple, Jr., *Digital Spectral Analysis with Applications* (Prentice Hall, New York, 1987).
13. Yu. E. Voskoboinikov, “Optimal parameter estimation of spatial-local signal filtering algorithms,” Optoelectron., Instrum. Data Process. **55**, 222–229 (2019). https://doi.org/10.3103/S8756699019030026
14. W. L. Pratt, *Digital Image Processing* (Wiley, New York, 1978).
15. L. Rabiner and B. Gold, *Theory and Application of Digital Signal Processing* (Prentice Hall, Englewood Cliffs, N.J., 1975).

Translated by O. Pismenov